

Enhancing Color Representation for the Color Vision Impaired

Jia-Bin Huang, Sih-Ying Wu, Chu-Song Chen

► **To cite this version:**

Jia-Bin Huang, Sih-Ying Wu, Chu-Song Chen. Enhancing Color Representation for the Color Vision Impaired. Workshop on Computer Vision Applications for the Visually Impaired, Oct 2008, Marseille, France. 2008. <inria-00321936>

HAL Id: inria-00321936

<https://hal.inria.fr/inria-00321936>

Submitted on 16 Sep 2008

HAL is a multi-disciplinary open access archive for the deposit and dissemination of scientific research documents, whether they are published or not. The documents may come from teaching and research institutions in France or abroad, or from public or private research centers.

L'archive ouverte pluridisciplinaire **HAL**, est destinée au dépôt et à la diffusion de documents scientifiques de niveau recherche, publiés ou non, émanant des établissements d'enseignement et de recherche français ou étrangers, des laboratoires publics ou privés.

Enhancing Color Representation for the Color Vision Impaired

Jia-Bin Huang¹, Sih-Ying Wu², and Chu-Song Chen¹

¹Institute of Information Science, Academia Sinica, Taipei, Taiwan

²Department of Electronics Engineering, National Chiao Tung University, Hsin Chu, Taiwan

Abstract. In this paper, we propose a fast re-coloring algorithm to improve the accessibility for the color vision impaired. Compared to people with normal color vision, people with color vision impairment have difficulty in distinguishing between certain combinations of colors. This may hinder visual communication owing to the increasing use of colors in recent years. To address this problem, we re-map the hue components in the HSV color space based on the statistics of local characteristics of the original color image. We enhance the color contrast through generalized histogram equalization. A control parameter is provided for various users to specify the degree of enhancement to meet their needs. Experimental results are illustrated to demonstrate the effectiveness and efficiency of the proposed re-coloring algorithm.

1 Introduction

Due to the availability of color printers and color display devices, the use of colors in multimedia contents to convey rich visual information has dramatically increased. It becomes more important to perceive colors for effective visual communication. However, people with certain types of color vision impairment have difficulty in distinguishing between some colors. In Fig. 1 we show examples of how color vision impaired people perceive color images. The two images in the left are the original color images perceived by people with normal vision, and the visual information can be easily interpreted. On the other hand, important color information in the original images may disappear or become indistinct in the six images in the right, which are the simulation results for people with different types of color vision deficiency (CVD).

In this paper, our aim is to resolve the potential inconsistency of visual perception between people with normal vision and people with CVD. We develop a fast algorithm to re-color images so that the original color contrast can be well preserved for color vision impaired viewers. Also, a user-specified parameter is provided for the trade-off between the enhancement degree and the naturalness in the re-colored images. We propose to re-map the hue components in the original color image through a spatially invariant global color transformation. The contrast is enhanced by forcing the confusing colors to have wider dynamic

ranges in the hue space. The luminance and the saturation components remain unaltered to ensure the naturalness of the re-colored image.

The remainder of this paper is structured as follows. Section 2 describes human visual color perception of colors and various types of CVD. In Section 3, we review previous works on re-coloring images for accommodating the color blindness. The proposed re-coloring algorithm is introduced in Section 4. Section 5 presents the experimental results, and Section 6 concludes this paper.

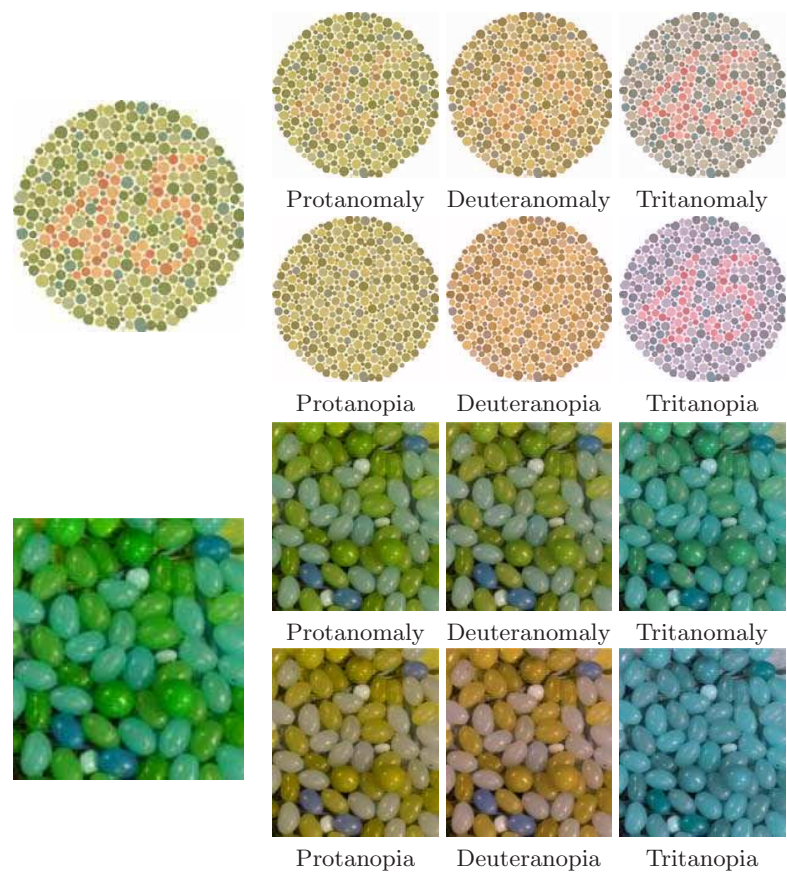


Fig. 1. Original color images and the simulation results for various types of color blindness. Images in the left are the original color images perceived by people with normal vision, while the six images in the right are the simulation results. The top row are the results for anomalous trichromacy and the bottom row are for dichromacy. From left to right, the first column is for protanopic viewers, the second is for deuteranopic viewers, and the third is for Tritanopic deficiency.

2 Color Vision Impairment

Normal color vision is based on the absorption of photons by three different types of fundamental photoreceptor cells, the *cone* cells. Three classes of cones have different spectral sensitivities with peak responses lying in the long- (L), middle- (M), and short- (S) wavelength regions of the spectrum, respectively. The energy received by the L, M, and S cones can be computed by a numerical integration over the wavelength λ :

$$[L, M, S] = \int E(\lambda)[\bar{l}, \bar{m}, \bar{s}]d\lambda, \quad (1)$$

where $E(\lambda)$ is the power spectral density of the light and $\bar{l}, \bar{m}, \bar{s}$ are the fundamental spectral sensitivity functions for L-, M-, and S-cones.

Color vision impairment, or *color vision deficiency*, results from partial or complete loss of function of one or more types of cone cells. There are three major types of CVD: anomalous trichromacy, dichromacy, and monochromacy, which are summarized in Table 1.

Anomalous trichromacy, a mild color deficiency, is often characterized by a shift of one of the three fundamental spectral sensitivity functions so that the pigments in one type of cones are not sufficiently distinct from the pigments in another type. The three types belonging to this category are protanomaly, deuteranomaly, and Tritanomaly, depending on deficiency (shift) in L-, M-, or S- cones.

A more severe color deficiency, dichromacy, is present when one of the three cone types is absent. Protanopia and deuteranopia, lacking L- and M-cones respectively, are unable to distinguish between colors in the green-yellow-red section of the spectrum, while those without S-cones are tritanopia that have difficulty in discriminating blue from yellow.

The last class is the severest but rarest type of CVD, called Monochromacy. Monochromats are also known as "total color blindness", lacking all types of cone cells. They are unable to distinguish any colors and can perceive brightness variations only.

There have been several works that attempt to simulate color deficient vision [1–3]. In [1], a computational model of CVD was formulated in the three dimensional LMS space, where three orthogonal axes L, M, and S represent the responses of the three different cones. The simulation algorithm computes the LMS tristimulus values from the RGB color space and projects colors in the LMS color space onto a pair of planes to represent the perceived responses by CVD viewers. The projected LMS values are then transformed to the RGB color space, allowing people with normal vision to experience how the CVD viewers perceive colors.

Fig. 1 shows examples of the simulation results of CVD. The top row in the two sets of images are the simulation results of anomalous trichromacy. Images listed from left to right are protanomaly, deuteranomaly, and tritanomaly. Similarly, the bottom row are results of dichromacy. Images listed from left

to right are the results of protanopia, deuteranopia, and tritanopia. The first image set is an image from Ishihara test chart. We can see that the number “45” disappears for protanopia and deuteranopia and become hard to recognize for protanomaly and deuteranomaly. The second image set contains blue-yellow content, which can not be distinguished by tritanopia.

With the ability to simulate color perception of CVD viewers, we can perform color transformation such that the color information in the original color images can be preserved for color-deficient users.

Table 1. Major genetic color deficiencies and prevalence for western races.

Type	Name	Cause of defect	Prevalence
Anomalous trichromacy	Protanomaly	L-cone defect	1.3%
	Deuteranomaly	M-cone defect	4.9%
	Tritanomaly	S-cone defect	0.01%
Dichromacy	Protanopia	L-cone absent	1%
	Deuteranopia	M-cone absent	1.1%
	Tritanopia	S-cone absent	0.002%
Monochromacy	Rod Monochromacy	no functioning cones	very rare

3 Related Work

Many previous works have been devoted to address CVD accessibility. We classify them into two main categories: 1) tools that provide guidelines for designers to avoid ambiguous color combinations, and 2) methods that (semi-)automatically reproduce colors that are suitable for CVD viewers.

Methods in the first category assist designers in color reproduction by providing guidelines [4], using a restricted CVD palette [5] [6], or verifying color schemes [7] [8]. However, it still takes a lot of effort for designers to select colors that are friendly for CVD viewers. Also, these methods can not be applied to existing natural images, which may contain tens of thousands of colors.

Based on the observation that red-green colorblind people (those with protanopic and deuteranopic deficiencies) are unable to distinguish between red and green, Daltonization [9] presents a procedure to allow users to specify three parameters for re-coloring images. The first parameter is for stretching contrast between red and green hues, the second one is for blue and yellow contrast modulation, and the last one is for modulating luminance component. The results are sensitive to the selection of the parameters. Improper parameters may result in unnatural images. Visual content adaptation for CVD viewers in the MPEG-21 digital item adaptation framework had been proposed in [10]. The adaptation for dichromats aims to provide better information by adjusting hue and saturation in the HSI color space. Ichikawa et al. [11] [12] proposed a more general method. First they used color quantization to select a subset of colors from the images,

and then build an objective function that maintains the color distances and the extent of re-coloring. They solved the optimization problem by a genetic search algorithm. The final result was obtained using an interpolation method. However, the lack of considering luminance consistency and the gamut constraint may raise some problems. Recently, Rasche et al. proposed automatic methods for re-coloring images using linear transformation [13] or constrained multidimensional scaling [14]. To alleviate the computational burden, 256 landmark colors are selected and used to minimize a pre-defined objective function, which preserves the proportional color differences. Unlike previous approaches focusing on re-coloring images only for CVD users, Huang et al. [15] aimed to maintain the naturalness of the original images as well as preserving the color contrasts. They constrained the color mapping as a rotation operation in the a^*b^* plane in the CIELab color space and introduced two objective functions: a detail term for CVD viewers and a naturalness term for normal views. A parameter was provided to control the trade-off between these two terms. In [16], Wakita et al. introduced three mapping errors to preserve the color information that the authors expect to convey in a document. They presented that color effects can be modeled as three types: color contrast, distinguishing ability, and natural coloring. However, the optimization process is very computational demanding and can only handle a small number of key colors (usually no more than 10). This prohibits the application for re-coloring natural images. Jefferson and Harvey [17] presented a framework for re-coloring color documents similar to [12], [14], and [15]. The novelties of their method lie in using the W3C color evaluation criteria, mapping without the gamut problem, and developing a new method for selecting key colors. Later in [18], they proposed an interface to assist CVD users to access digital images. The main idea is to transfer the color information of the defective cones to the working ones

One major disadvantage of the previous re-coloring methods through optimization approaches is the expensive computational cost. Moreover, the optimal results for the pre-defined objective functions may not necessarily yield visual appealing images for CVD viewers due to the luminance consistency or gamut mapping problems.

4 The Proposed Re-coloring Algorithm

4.1 Design Objectives

To address the problems stated in Section 3, we propose a fast approach that automatically enhances the color contrast for CVD viewers. Listed below are the three design objectives of our method:

1. Maintaining luminance and saturation consistency:
Our method aims not to enhance the contrast in the original image, but to maintain the contrast that may not be perceived by CVD users. The consistency of luminance and saturation is important to generate a natural image for people with normal vision.

2. Preserving the order of the hue:
By “the order of hue” we mean the ordering in the hue component in the HSV color space. In other words, we wish not to corrupt the natural hue ordering of the original image, but to stretch or compress the distance between them.
3. Fast computation:
We aim to design a fast algorithm that is applicable to real-time applications.

Since the luminance and saturation components are often not the major factors that lead to confusion for CVD users, we choose the simplest way to preserve them: leave them unchanged. An RGB color images is first converted to the HSV color space and then we apply a color transfer function to the hue component only. To preserve the natural ordering of hue, the hue transfer function is constrained to be a non-decreasing function. In the next subsection, we show how the hue transfer function can be obtained without performing a time-consuming optimization procedure. After transferring the hue values, the re-colored image is converted back to the RGB color space for display.

4.2 Re-coloring using Generalized Histogram Equalization

We enhance the contrast in the hue channel through a histogram transformation approach. Histogram equalization (HE) is one of the most well-known techniques for image enhancement. HE enhances the contrast of an image by expanding the dynamic range of the original image such that the histogram of the resultant image is better distributed. To this end, the cumulative density function is used for intensity mapping.

The intensity transfer function is found by first generating the histogram of the image, and then the mapping function can be written as:

$$T(g) = g_{min} + (g_{max} - g_{min}) \int_{g_{min}}^g \overline{hist}(g) dg, \quad (2)$$

where the $\overline{hist}(g)$ is the normalized histogram, g is the original intensity value, and g_{max} and g_{min} are the maximum and minimum intensity values of g , respectively. The normalized histogram $\overline{hist}(g)$, that is, the probability distribution of the grey levels in an image, can also be interpreted as an expansion function, where a larger value of $\overline{hist}(g)$ tends to stretch the range of grey levels around g . Since the histogram only contains the global statistics (the occurrence frequency of each grey level) of an image, unexpected effects like over-enhancement may occur in some regions because local characteristics are not considered. Therefore, we adapt the generalized histogram equalization (GHE) [19] to our re-coloring algorithm.

The generation of the histogram in HE is a masking-and-accumulating operation with 1×1 window. In the GHE, the mask is generalized from 1×1 to $n \times n$ to encode the local information into the histogram. We use a 3×3 mask for simplicity, and in practice larger masks like 5×5 or 7×7 do not affect the results significantly.

We measure three local characteristics α , β , and γ within the neighborhood system $N(x, y)$ centered at point (x, y) . The first measurement α is the hue value at point (x, y) , which is the only measurement in HE:

$$\alpha(x, y) = hue(x, y). \quad (3)$$

The second one β measures the maximum local hue difference within the neighborhood system $N(x, y)$:

$$\beta(x, y) = \max_{i,j} \{hue(i, j)\} - \min_{i,j} \{hue(i, j)\}, (i, j) \in N(x, y). \quad (4)$$

Obviously, more complicated measurement like local hue variance can be used as well. The last one evaluates the local color information loss due to CVD in the CIELab color space, where the Euclidian distance corresponds to human visual perception of color difference:

$$\gamma(x, y) = \sum_{(i,j) \in N(x,y)} (||C(x, y) - C(i, j)|| - ||Sim(C(x, y)) - Sim(C(i, j))||)^2, \quad (5)$$

where $C(x, y)$ is the CIELab color at point (x, y) , $|| \cdot ||$ is the Euclidean norm, and $Sim(\cdot)$ is the simulation CIELab color for CVD viewers [1].

The third measurement γ evaluates how much local color contrast is lost when the image is perceived by CVD viewers. One can expect that γ has a large value in regions where color confusion occurs. We show in Fig. 2(a) a natural image with red and green colors. In Fig. 2(b), the color contrast between red and green is lost when perceived by protanopia. Fig. 2(c) illustrates the map of γ values in logarithmic scale. The brighter regions correspond to larger γ values.



Fig. 2. The information loss map in image “berries”. (a) The original color image. (b) The simulation result for protanopia. (c) The local color contrast loss map in logarithmic scale.

The expansion function from a pixel in HE is a dirac delta function $\delta(x - g)$, while in GHE, the expansion function can be conditional on the measured local characteristics, and common kernel functions such as Gaussian, Rectangle and

Epanechnikov can be used. With the computational efficiency in mind, we choose the rectangle kernel as our expansion function:

$$S(h|\alpha, \beta, \gamma) = \gamma \times \text{Rect}\left(\frac{h - \alpha}{\beta}\right), \quad (6)$$

where the $\text{Rect}(\cdot)$ is the rectangle kernel which can be expressed as:

$$\text{Rect}(x) \equiv \begin{cases} 1, & \text{if } -0.5 \leq x \leq 0.5, \\ 0, & \text{otherwise.} \end{cases} \quad (7)$$

After scanning over the input color image, calculating the local characteristics, the generalized histogram $GH(h)$ can be obtained:

$$GH(h) = \int \int S(h|\alpha(x, y), \beta(x, y), \gamma(x, y)) dx dy, \quad (8)$$

Similar to HE, we can then construct the hue transfer function $T(h)$:

$$T(h) = h_{min} + (h_{max} - h_{min}) \int_{h_{min}}^h \overline{GH}(h) dh, \quad (9)$$

where h denotes the input hue value. Note that the transfer function is always non-negative and non-decreasing, and thus can yield more visual pleasing images. The h_{min} is not altered after the hue transfer function $h_{min} = T(h_{min})$. Since the hue axis is circular, users can specify a pivot hue value so that this hue value will not be changed after enhancing. In this paper, h_{min} is set to be zero.

4.3 Controlling the Degree of Enhancement

Although the hue transfer function can be automatically computed from the given image, we provide a parameter for users to control the degree of enhancement to satisfy various needs of different viewers. This is achieved by introducing a magnitude mapping function:

$$M(x) = x^p, \quad (10)$$

where p is a user-specified control parameter. The transfer function is further modified as:

$$T(h) = h_{min} + (h_{max} - h_{min}) \frac{\int_{h_{min}}^h M(\overline{GH}(h)) dh}{\int_{h_{min}}^{h_{max}} M(\overline{GH}(h)) dh}. \quad (11)$$

If p is larger than one, the normalized expansion function is emphasized, resulting in more significant enhancement. If users prefer to generate a more natural image, $p < 1$ can be specified so that the dynamic range of the normalized expansion function is compressed. Note that if $p = 0$, the transfer function maps every input value to itself, generating the original image.

5 Results and Discussion

We have implemented and tested our algorithm using C++ on a Pentium 4 3.4GHz PC. The complexity of our algorithm scales linearly with the size of the input image. Re-coloring an image with 200x200 pixels takes less than 0.5 second, which is significantly faster than previous published works (a few minutes or more [17] [13] [14]).

Since it is difficult to gather various types of color-deficient viewers to evaluate our method, we use the computational model to simulate color perception of people with CVD. We use the images from the Ishihara test chart to demonstrate the effectiveness of the proposed re-coloring method. Ishihara test chart is a book that consists of a number of cards for discovering congenital color blindness and red-green blindness. Two samples from Ishihara test chart are shown in the left of Fig. 3. People with normal vision can easily identify the number “6” and “8” in the original images. However, people with dichromacy are unable to see the number from the test chart (simulated in Fig. 3(a)(b)), while the numbers are very unclear to those with anomalous trichromacy (simulated in Fig. 3(e)(f)). We apply our re-coloring algorithm to these two test charts. The re-colored and simulated results for different types of CVD are shown in Fig. 3 (c)(d)(g)(h). After re-coloring, we can see that the numbers appear (for dichromacy) or become clearer (for anomalous trichromacy) for CVD viewers.

We compare our algorithm with that proposed by Rasche et al. in [14]. The left part of Fig. 4 is the simulation result for protanopia and the right part are for deuteranopia. Fig. 4 (a) (d) show the simulation results for protanopia and deuteranopia, respectively. The re-colored and simulated images by our method are shown in Fig. 4 (b) (e). Fig. 4 (c) (f) show the results by Rasche et al. Their method did generate images with high contrast, but may yield over-enhanced images because they did not take hue order preserving into consideration. Note also that, their method maps the green to blue in the upper image “berries” and maps the red to blue in the lower image “flower”. This causes no problems in still images, but may result in corruption of temporal coherence in videos.

Fig. 5 shows the comparison with method proposed by Jefferson et al. in [17]. Fig. 5(a) are the two original color image, which contain coloring pencils. The simulated images for deuteranopia (in the left) and tritanopia (in the right) are illustrated in Fig. 5(b). We can see that the color contrast in the original image disappears when perceived by CVD users. Fig. 5(c) (e) show the re-colored images by our approach and by Jefferson et al.’s method, respectively. The corresponding simulation results of the re-colored images are shown in Fig. 5(d) (f). The images re-colored by Jefferson et al.’s method are unnatural, and the luminance of the re-colored images are inconsistent with the original ones. Compared with their method, our re-coloring algorithm produces more perceptually pleasing images.

We also show the effects caused by the control parameter p . A natural image “flower” and an image taken from Ishihara test chart are re-colored using different parameter p . Fig. 6(a) (b) show the original images and their simulation results for deuteranopia. From Fig. 6(c) to (h), the control parameter p is set

from 0.2 to 1.2, with an increasing step 0.2. As p increases, the simulated image exhibits higher contrast, which is particularly obvious in the test chart images.

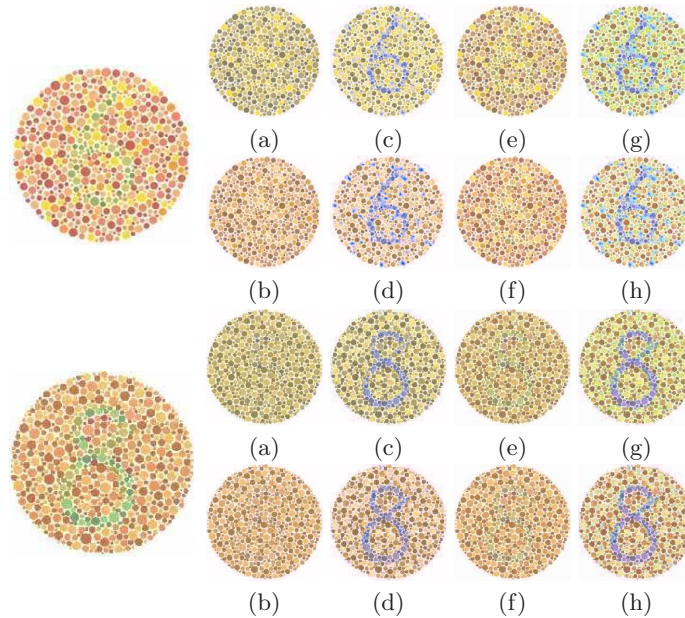


Fig. 3. Enhancing color contrast for red-green types of CVD on images from Ishihara test chart. (a)(b) The simulation results for protanopia and deuteranopia, respectively. (c)(d) The simulation results of the re-colored images for protanopia and deuteranopia. (e)(f) The simulation results for protanomaly and deuteranomaly, respectively. (g)(h) The simulation results of the re-colored images for protanomaly and deuteranomaly.

6 Conclusions

In this paper, we have proposed a fast and effective re-coloring algorithm for people with color vision impairment. We propose to enhance the contrast in the hue channel only, which is the major factor resulting in confusion in visual communication. We employ the generalized histogram technique to encode local information in the original color image. We also provide a control parameter for users to specify the degree of enhancement. Our algorithm can run at real-time, and thus can be easily extended to video processing applications. Computational simulation results have demonstrated the effectiveness and efficiency of the proposed algorithm.

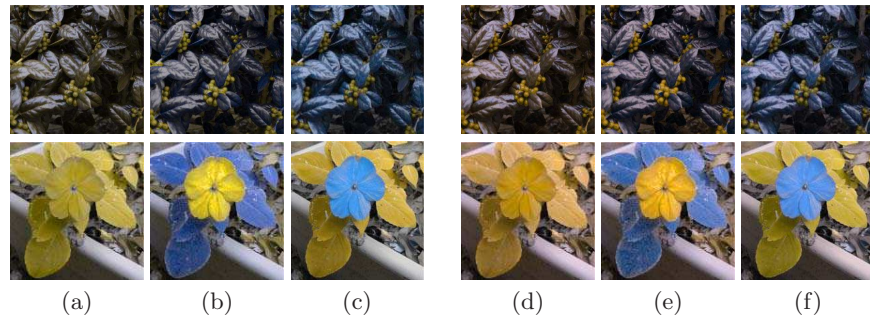


Fig. 4. Comparison with Rasche et al.'s method using two images “berries” and “flower”. The left part are the simulation results for protanopia and the right image set is the simulated images for deuteranopia. (a)(d) Simulated images. (b)(e) Simulation results of the re-colored images by our method (with $p = 0.6$). (c)(f) Simulation results of the re-colored images by our method by Rasche et al.'s method.

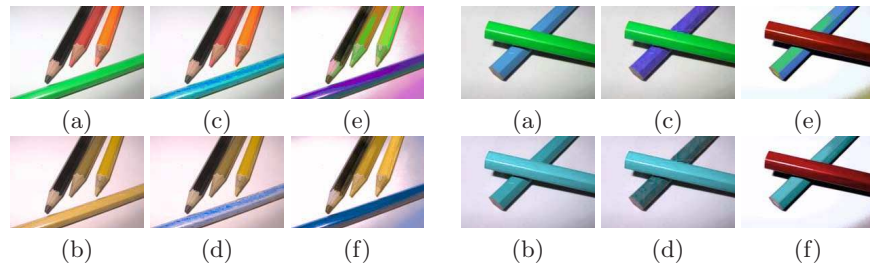


Fig. 5. Comparison with Jefferson et al.'s method. The left image set is for deuteranopia, and the right image set is for tritanopia. (a) The original color image. (b) The simulated image. (c) Re-colored image using the proposed algorithm ($p=0.6$). (d) Simulation result of (c). (e) Re-colored image using Jefferson et al.'s method. (f) Simulation result of (e).

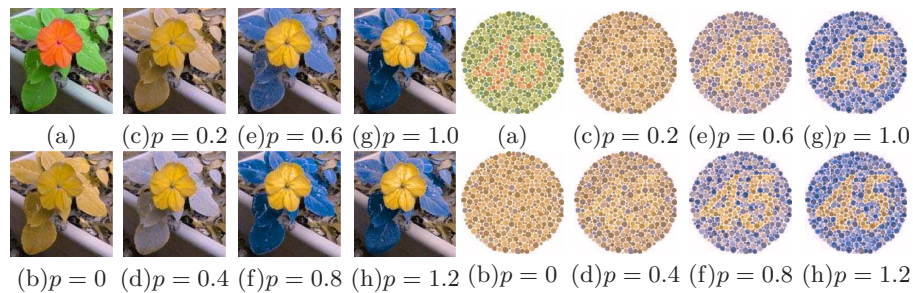


Fig. 6. Controlling the degree of enhancement by the control parameter p . (a) The original color image. (b) Simulation result for deuteranopia after re-coloring with $p = 0$. (c)-(f) The simulated images of the re-colored images using various parameters p .

Acknowledgement

This research was supported by the National Science Council of Taiwan under Grant No. NSC 96-3113-H-001-011.

References

1. Brettel, H., Viénot, F., Mollon, J.: Computerized simulation of color appearance for dichromats. *Journal of the Optical Society of America A* **14** (1997) 2647–2655
2. Kondo, S.: A computer simulation of anomalous color vision. (*Color Vision Deficiencies*) 145–159
3. Meyer, G., Greenberg, D.: Color-defective vision and computer graphics displays. *IEEE Computer Graphics and Applications* **8** (1988) 28–40
4. Chisholm, W., Vanderheiden, G., Jacobs, I.: Web content accessibility guidelines 1.0. *interactions* **8** (2001) 35–54
5. Rigden, C.: The Eye of the Beholder-Designing for Colour-Blind Users. *British Telecommunications Engineering* **17** (1999) 3
6. Viénot, F., Brettel, H., Mollon, J.: Digital video colourmaps for checking the legibility of displays by dichromats. *Color Research and Application* **24** (1999) 243–252
7. Walraven, J., Alferdinck, J.: Color displays for the color blind. *IS&T and SID 5th Color Imaging Conference* (1997) 17–22
8. Jenny, B., Kelso, N.: Designing Maps for the Colour-Vision Impaired. *Cartographic Perspectives* (2007) 61–67
9. Dougherty, R., Wade, A.: Daltonize. (<http://www.vischeck.com/daltonize/>)
10. Song, J., Yang, S., Kim, C., Nam, J., Hong, J., Ro, Y.: Digital item adaptation for color vision variations. *Proceedings of SPIE* **5007** (2003) 96
11. Ichikawa, M., Tanaka, K., Kondo, S., Hiroshima, K., Ichikawa, K., Tanabe, S., Fukami, K.: Web-Page Color Modification for Barrier-Free Color Vision with Genetic Algorithm. *LNCS* **2724** (2003) 2134–2146
12. Ichikawa, M., Tanaka, K., Kondo, S., Hiroshima, K., Ichikawa, K., Tanabe, S., Fukami, K.: Preliminary study on color modification for still images to realize barrier-free color vision. In: *IEEE Int'l Conf. on SMC*. Volume 1. (2004)
13. Rasche, K., Geist, R., Westall, J.: Detail Preserving Reproduction of Color Images for Monochromats and Dichromats. *IEEE Computer Graphics and Applications* **25** (2005) 22–30
14. Rasche, K., Geist, R., Westall, J.: Re-coloring Images for Gamuts of Lower Dimension. *EuroGraphics* **24** (2005) 423–432
15. Huang, J.B., Tseng, Y.C., Wu, S.I., Wang, S.J.: Information Preserving Color Transformation for Protanopia and Deuteranopia. *IEEE Signal Processing Letters* **14** (2007) 711–714
16. Wakita, K., Shimamura, K.: SmartColor: Disambiguation Framework for the Colorblind. In: *ACM Assets*. (2005) 158–165
17. Jefferson, L., Harvey, R.: Accommodating color blind computer users. In: *ACM SIGACCESS conf. on Computers and accessibility*. (2006) 40–47
18. Jefferson, L., Harvey, R.: An interface to support color blind computer users. In: *SIGCHI conf. on Human factors in computing systems*. (2007) 1535–1538
19. Jen, T.C., Wang, S.J.: Generalized Histogram Equalization Based on Local Characteristics. In: *proc. ICIP*. (2006) 2877–2880